

PAPER • OPEN ACCESS

# Mechanical, thermal and rheological characterization of polystyrene/organoclay nanocomposites containing aliphatic elastomer modifiers

To cite this article: Ali Sinan Dike and Ulku Yilmazer 2020 *Mater. Res. Express* 7 015055

View the [article online](#) for updates and enhancements.

## Recent citations

- [Evaluation of water repellency in bentonite filled polypropylene composites via physical and mechanical methods](#)  
Oyku Yildirimkaraman *et al*

The banner features a background image of Earth from space. On the left, there are three circular logos: the top one is 'ECS' in a circle, the middle one is 'The Electrochemical Society' with a stylized 'ECS' logo, and the bottom one is 'THE KOREAN ELECTROCHEMICAL SOCIETY'. The main text in the center reads: 'The best technical content in electrochemistry and solid state science and technology!'. Below this, a blue bar contains the text 'Available until November 9, 2020.'. On the right side, there is a logo for 'PRIME™ PACIFIC RIM MEETING ON ELECTROCHEMICAL AND SOLID STATE SCIENCE 2020'. At the bottom right, a dark blue box contains the text 'REGISTER TO ACCESS CONTENT FOR FREE!' with a right-pointing arrow.

# Materials Research Express



## PAPER

# Mechanical, thermal and rheological characterization of polystyrene/organoclay nanocomposites containing aliphatic elastomer modifiers

### OPEN ACCESS

RECEIVED  
6 October 2019

REVISED  
17 December 2019


ACCEPTED FOR PUBLICATION  
2 January 2020

PUBLISHED  
13 January 2020

Original content from this work may be used under the terms of the [Creative Commons Attribution 4.0 licence](#).

Any further distribution of this work must maintain attribution to the author(s) and the title of the work, journal citation and DOI.



Ali Sinan Dike<sup>1</sup>  and Ulku Yilmazer<sup>2,3</sup>

<sup>1</sup> Materials Engineering, Adana Alparslan Turkes Science and Technology University, Adana, Turkey

<sup>2</sup> Chemical Engineering, Middle East Technical University, Ankara, Turkey

<sup>3</sup> Polymer Science and Technology, Middle East Technical University, Ankara, Turkey

E-mail: [yilmazer@metu.edu.tr](mailto:yilmazer@metu.edu.tr)

**Keywords:** polystyrene, nanocomposites, extrusion, aliphatic elastomer, organoclay

## Abstract

In this study, organoclay containing polystyrene (PS) based nanocomposites were prepared by extrusion in the presence of aliphatic elastomer modifiers. Three different types of aliphatic elastomeric materials and three different types of organoclays were used. Their effects on the morphology, and mechanical, thermal, and rheological properties of PS were investigated by scanning electron microscopy (SEM), transmission electron microscopy (TEM) and x-ray diffraction (XRD), tensile and impact tests, differential scanning calorimetry (DSC), and melt flow index measurements, respectively. Lotader AX8900, Lotader AX8840 and Lotader 2210 were chosen as the aliphatic elastomeric compatibilizers; and Cloisite 15 A, Cloisite 25 A and Cloisite 30B were chosen as the organoclays. The organoclay content was kept constant at 2 wt% and elastomer content was kept constant at 5 wt% throughout the study. Significant improvement is observed on the basal spacing for 30B containing samples according to XRD analysis. SEM studies indicate that the clay particles mostly reside between the PS matrix and the spherical elastomeric domains. Additions of elastomer and organoclay decrease the MFI value of PS. Mechanical test results show that, improvement is observed in elongation at break of unfilled PS with the addition of elastomers. Organoclay addition increases the tensile modulus of PS. According to thermal characterizations, the glass transition temperature ( $T_g$ ) of PS decreases with elastomer addition, whereas organoclay addition shifts  $T_g$  values to higher temperatures.

## 1. Introduction

Nanocomposites are a class of plastic compounds containing well dispersed and exfoliated nanofillers such as nanoclays. Due to the structural properties gained by well dispersion of the nanosized fillers, nanocomposites possess highly improved mechanical, thermal, physical, and barrier properties when compared to pristine polymer and conventional composites [1, 2]. Layered silicates are widely used in nanocomposites as inorganic fillers, and they have high aspect ratios. Material properties improve significantly in the case of well dispersion of the silicate layers throughout the polymer matrix owing to interaction of the filler and the polymer. Montmorillonite which belongs to the general family of 2:1 layered silicate is the most commonly used smectite clay in nanocomposites. The structure of montmorillonite consists of an octahedral alumina sheet between two tetrahedral silica sheets. The layer thickness of the crystal structure is around 1 nm, and the lateral dimensions of these layers may be in the range of 30 nm to several microns or larger [3–8].

Polystyrene (PS) is one of the most widely used kind of plastic. PS is a versatile polymer whose principal characteristics include transparency, ease of coloring and processing, and low cost. Because of the brittle characteristics of polystyrene, the main development directions were aimed at copolymerization of styrene with polar co-monomers such as methacrylates or maleic anhydride and elastomeric modifiers [9–11]. In order to

provide well dispersion of organoclay in PS matrix, a third material may be used in nanocomposites, called as compatibilizer.

There are some studies in the literature that emphasize the effect of the compatibilizer on dispersion of organoclay in the PS matrix. Park *et al* processed PS/organoclay nanocomposites in the presence of poly (styrene-co-vinylloxazolin) (OPS). They found out that the arrangement of the organic modifier between the clay layers affects the dispersion of layers [12]. Zhang *et al* synthesized PS-clay nanocomposites by  $\gamma$ -radiation technique using four different modified clays. Three of the modified clays were reactive while one was non-reactive. With the reactive modified clays, exfoliated structures were obtained, whereas with the nonreactive clay intercalated structure was obtained. The thermal properties of nanocomposites prepared by reactive clay were greatly enhanced due to the chemical bond formed between the clay and the chains of PS [13]. Xie *et al* prepared PS-clay nanocomposites by suspension polymerization of styrene monomer in the presence of organoclay and investigated the effects of organoclay concentration and alkyl chain lengths of surfactants on the properties of PS-clay nanocomposites. They postulated that nanocomposite with the highest glass transition temperature was obtained as the surfactant possessing the highest chain length [14]. Tanoue *et al* demonstrated that the dispersion of silicate layer for PS/organoclay nanocomposites were affected by the processing conditions such as screw rotation speed [15]. Doh and Cho investigated the effects of various o-MMT structures on the properties of PS-MMT nanocomposites. They indicated that nanocomposite containing benzyl unit, similar to styrene monomer, in o-MMT exhibited the highest decomposition temperature [16]. Gilman *et al* prepared nanocomposites using modified fluorohectorite and montmorillonite by melt intercalation and they confirmed that it is a neatly intercalated structure [17]. Fu *et al* synthesized PS-clay nanocomposites by direct dispersion of organically modified clay in styrene monomer followed by free-radical polymerization, and they stated that vinyl benzyl group of the surfactant is effective in exfoliating MMT in PS matrix [18]. Zhang *et al* reported the first example of clay that contains a carbocation and its use to prepare PS-clay nanocomposites. The nanocomposite was prepared by emulsion polymerization and its mixed intercalated-exfoliated structure was established by XRD [19].

The aim of this study is to investigate the effects of compatibilizer type and organoclay type on the morphology, mechanical, thermal and rheological properties of polystyrene. Three types of compatibilizers, terpolymer of ethylene–methyl acrylate–glycidyl methacrylate (E-MA-GMA), copolymer of ethylene-glycidyl methacrylate (E-GMA), and terpolymer of ethylene–n-butyl acrylate–maleic anhydride (E-nBA-MAH), and organoclays, Cloisite 15 A, Cloisite 25 A and Cloisite 30B were used. First, PS/compatibilizer blends containing 5 wt% of compatibilizer were prepared by means of a co-rotating twin screw extruder. Then, ternary nanocomposites containing 5 wt% of compatibilizer and 2 wt% of organoclay were produced similarly by twin screw extrusion. In order to characterize the nanocomposites, all standard test specimens were prepared by injection molding. X-Ray diffraction (XRD) analyses were performed in order to observe the dispersion of the organoclay in the matrix. Scanning electron microscopy (SEM) analysis was performed to observe the dispersion of elastomeric phase and effects of organoclay on domain sizes. Thermal characterization of the nanocomposites was performed by differential scanning calorimetry (DSC). Flow properties were determined by melt flow index (MFI) measurements, and mechanical characterizations of the nanocomposites were performed by tensile and impact tests.

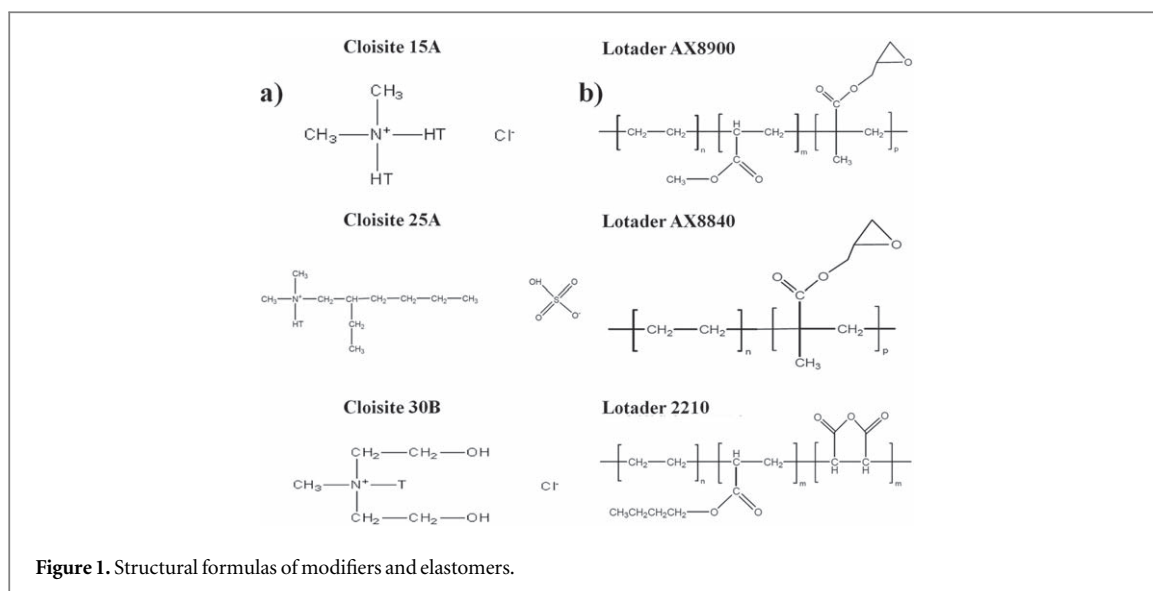
## 2. Experimental

### 2.1. Materials

PS with a trade name of Lacqrene<sup>®</sup> 1960N was used. It was purchased from Total Petrochemicals, USA and supplied in the form of pellets in 25 kg polyethylene bags. Three different montmorillonites modified with quaternary ammonium salts were used in this study as fillers. These organoclays, namely Cloisite<sup>®</sup> 15 A, Cloisite<sup>®</sup> 25 A, and Cloisite<sup>®</sup> 30B, were purchased from Southern Clay Products, Texas, USA. Aliphatic elastomers, Lotader<sup>®</sup> AX8900, a terpolymer of ethylene–methyl acrylate–glycidyl methacrylate (E-MA-GMA); Lotader<sup>®</sup> AX8840, a copolymer of ethylene–glycidyl methacrylate (E-GMA), and Lotader<sup>®</sup> 2210, a terpolymer of ethylene–nbutyl acrylate–maleic anhydride (E-nBA-MAH), were chosen as the compatibilizers. The structural formulas of the organic modifiers of Cloisite 15 A, Cloisite 25 A and Cloisite 30B are shown in figure 1(a). The structural formulas of Lotader<sup>®</sup> AX8900, Lotader<sup>®</sup> AX8840, and Lotader<sup>®</sup> 2210 are shown in figure 1(b). All of the elastomers were purchased from Arkema Inc., France.

### 2.2. Preparation of the composites

A co-rotating twin screw extruder was used in order to obtain the ternary nanocomposites. The model of the extruder is Thermoprism TSE 16 TC with L/D = 24. The screw diameter and the twin bore diameter of the extruder are 15.6 mm and 16 mm respectively. It has a barrel length of 384 mm. In addition to these, maximum



screw speed and maximum torque that can be achieved are 500 rpm and 12 Nm. During the extrusion process, temperature profile of the hopper, the mixing zones and the die, the screw speed, and the total flow rate of feed were kept constant. Process temperatures were 30, 200, 200, 200, 200 °C for the hopper, the three mixing zones and the die, respectively. The screw speed and total flow rate of feed were kept constant at 150 rpm and 25 g min<sup>-1</sup> throughout the process. In order to obtain the desired compositions, inlet flow rate of the main-feeder and the side-feeder were calibrated before each extrusion run. The molten product obtained from the extruder barrel was cooled by passing through a water bath, whose temperature was continuously controlled. At the end of the water bath, a blower was placed in order to remove the water from the product surface, and finally the product was collected in plastics bags after passing through the pelletizer. After the extrusion, the specimens were injection molded by DSM Xplore laboratory scale micro injection molding equipment. During the molding process, the melt and mold temperatures were set to 200 °C and 30 °C, respectively for all the samples.

### 2.3. Characterization techniques

The composites containing organoclay were analyzed by using a Rigaku D/Max 2200/PC x-ray diffractometer that generates a voltage of 40 kV and current of 40 mA from Cu K $\alpha$  radiation source ( $\lambda = 1.5418$ ). The diffraction angle  $2\theta$  was scanned from 1° to 10° with scanning rate of 1°/min and a step size of 0.02°. Bragg's law was used to calculate the distance between the silicate layers. The samples for XRD analyses were obtained from injection molded specimens. SEM analysis was performed by a JEOL JSM-6400 low voltage scanning electron microscope. The impact fracture surfaces were etched in an ultrasonic bath for 15 min at 30 °C, by using n-heptane to dissolve the elastomeric phase. Before SEM photographs were taken, the fractured surfaces were coated with a thin layer of gold in order to obtain a conductive surface. SEM photographs were taken for each specimen at x250 and x1500 magnifications. This analysis was used to observe the dispersion of the elastomeric phase and investigate the failure mechanism of the nanocomposites and blends. In order to perform TEM analysis, nanocomposite samples having 70 nm thickness were cut cryogenically, at a temperature of -100 °C, using a diamond knife. Test samples were examined by a FEI Transmission Electron Microscope at an acceleration rate of 80 kV during the TEM study. The glass transition temperature measurements of the samples were carried out under nitrogen atmosphere by using Perkin Elmer Diamond differential scanning calorimeter. The samples were heated from 20 °C to 350 °C with a heating rate of 20 °C min<sup>-1</sup>. Tensile tests were performed for each composition according to ASTM D638M-91a using a Lloyd LR 30 K universal Testing machine. The crosshead speed was calculated as 3 mm min<sup>-1</sup>, based on the gauge length of 30 mm and strain rate of 0.1 min<sup>-1</sup>. The test was performed by pulling the specimens until failure. Stress and strain data were obtained from the mechanical testing device, and tensile strength, tensile modulus, strain at yield and strain at break values were determined by using these graphs. In order to perform impact test, samples with dimensions of 80 × 10 × 4 mm were used with a Ceast Resil Impactor. All of the tests were performed at room temperature. At least five samples were used for each composition set, and the average and standard deviation values were calculated. MFI test was performed according to ASTM D1238-79 using an Omega Melt Flow Indexer. The measurements were carried out at 200 °C with a load of 2.16 kg. The weight of the sample passing through the die in 10 min, defined as the melt index, was determined for all the compositions. At least five measurements were done for each sample to get accurate results. The results were recorded as g/10 min.

**Table 1.** XRD results of all the compositions.

Composition	1st peak		2nd peak	
	2theta (°)	d <sub>001</sub> (Å)	2theta (°)	d <sub>001</sub> (Å)
15 A	2.80	31.5	7.10	12.4
25 A	4.72	18.7	—	—
30B	4.88	18.1	—	—
PS + 15 A	2.87	30.7	5.56	15.9
PS + 25 A	3.28	26.9	5.62	15.7
PS + 30B	6.00	14.7	—	—
PS + 2210 + 15 A	2.79	31.7	5.15	17.2
PS + 2210 + 25 A	3.13	28.2	5.67	15.6
PS + 2210 + 30B	6.20	14.3	—	—
PS + 8840 + 15 A	2.57	34.4	5.10	17.3
PS + 8840 + 25 A	2.83	31.2	5.37	16.5
PS + 8840 + 30B	6.23	14.2	—	—
PS + 8900 + 15 A	2.36	37.4	4.52	19.6
PS + 8900 + 25 A	2.56	34.5	—	—
PS + 8900 + 30B	2.09	42.3	6.24	14.2

### 3. Results and discussion

#### 3.1. XRD study

XRD analysis has been widely used to analyze the dispersion state of an organoclay in the polymer matrix and the interlayer spacing of the silicate layers. The intercalation of polymer chains between the silicate layers results in an increase in the interlayer spacing. For intercalated structures, the characteristic peak tends to shift to a lower angle due to the expansion of the basal spacing [20–22]. Although the layer spacing increases, there still exists an attractive force between the layers to stack them in an ordered structure. Change in intensity and the shape of the basal reflections is another evidence that specifies the intercalation of polymer chains [23, 24].

The basal spacing values of all the compositions are shown in table 1. The basal spacing of the organoclays 30B, 15 A and 25 A were found as 18.1 Å, 31.5 Å–12.4 Å and 18.7 Å respectively. The secondary peak d<sub>002</sub> in 15 A is attributed to unmodified clay, since it coincides with the d-spacing of unmodified clay. XRD patterns of binary PS/organoclay nanocomposites are shown in figure 2(a). The basal spacing of the silicate layers in binary nanocomposites decreased with respect to the basal spacing of layers in original powders of 15 A and 30B. The change in the d<sub>001</sub> interlayer spacing of the binary nanocomposite containing 15 A is not significant. However, due to insertion of the PS chains between unmodified layers, the second peak is shifted to the left. There are many parameters which may affect exfoliation of clay layers such as polarity, shear intensity of the extruder, initial d-spacing value, organoclay stability and surfactant packing density. 15 A has the most hydrophobic surface and the highest initial d-spacing value among the organoclays due to absence of polar groups on its modifier. Attraction between platelets in 15 A is relatively low due to high interlayer spacing, and diffusion of polymer chains into these layers might be easier. Thus, it is expected that interaction between non-polar polystyrene matrix and 15 A should be higher than the other organoclays. In spite of this high interaction, other factors restrict the exfoliation of the clay platelets. 15 A has two long aliphatic tails and these tails may restrict the access of polymer chains to the clay surface. Because of these alkyl chains, the interaction between the platelets of Cloisite 15 A and polymer chains could not be overcome. 30B has the most hydrophilic surface among the organoclays owing to the hydroxyl groups on its organic modifier. Thus, its dispersion is poor in the highly non-polar PS matrix. However, in 25 A the d<sub>001</sub> peak of the powder increased from 18.7 Å to 26.9 Å upon compounding with PS. Also, another peak appeared at 15.7 Å. This is probably arising from unintercalated clay layers of 25 A. The intercalation and/or exfoliation of polystyrene chains was tried to be achieved by adding a third component to the PS/organoclay binary nanocomposites.

Figures 2(b)–(d) show the XRD patterns of the nanocomposites containing organoclays and elastomers. When the effects of organoclay and elastomer type on the dispersion of silicate layers are investigated, little enhancement can be observed in the basal spacing of these ternary nanocomposites. Besides, in some cases the diffraction peak shifted to the right, indicating a decrease in the basal spacing. In general, addition of elastomeric compatibilizers 2210 and 8840 had little positive effect on the intercalation or exfoliation of silicate layers. The interaction between the functional groups of the elastomeric materials and hydroxyl groups on the clay surface may be weakened due to heat treatment or the decomposition of organic modifier, so that some portion of the ammonia salts may have exuded from the clay gallery, leading to a decrease in interlayer spacing

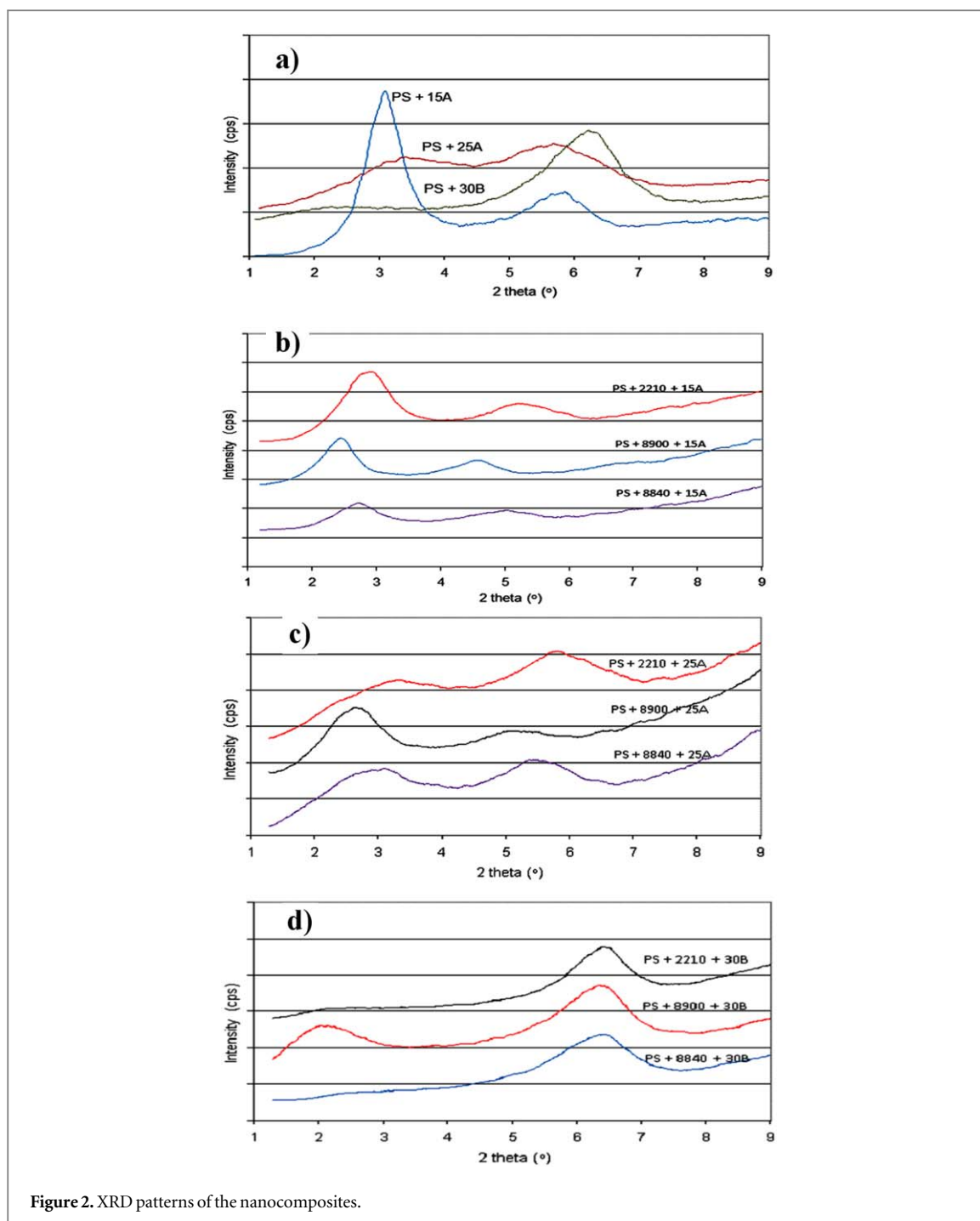


Figure 2. XRD patterns of the nanocomposites.

[25, 26]. Another reason of the collapse in basal spacing may be explained by the applied high pressure during the injection molding process [27]. In the injection molding process, molten polymer is injected from the barrel to the mold by applying about 10 bars of pressure. High pressure may also cause the reduction in the basal spacing of the silicate layers.

Lotader<sup>®</sup> AX8900 is observed to be the most effective compatibilizer in intercalating and/or exfoliating the organoclay layers, especially when it is used with the organoclay 30B. Both Lotader<sup>®</sup> AX8900 and Lotader<sup>®</sup> AX8840 have the reactive epoxy group that can react with the hydroxyl group on Cloisite<sup>®</sup> 30B, and thus intercalate the clay layers. Also, in comparison to Lotader<sup>®</sup> AX8840, Lotader<sup>®</sup> AX8900 has the methyl acrylate group that increases the polarity of the compatibilizer and provides higher attraction with the polar organoclay Cloisite<sup>®</sup> 30B.

### 3.2. SEM and TEM analyses

The fracture surface of the composites and blends were examined by SEM analysis for investigation of elastomer and organoclay inclusions on the morphology of PS. Image J software was used to analyze the dispersion of the

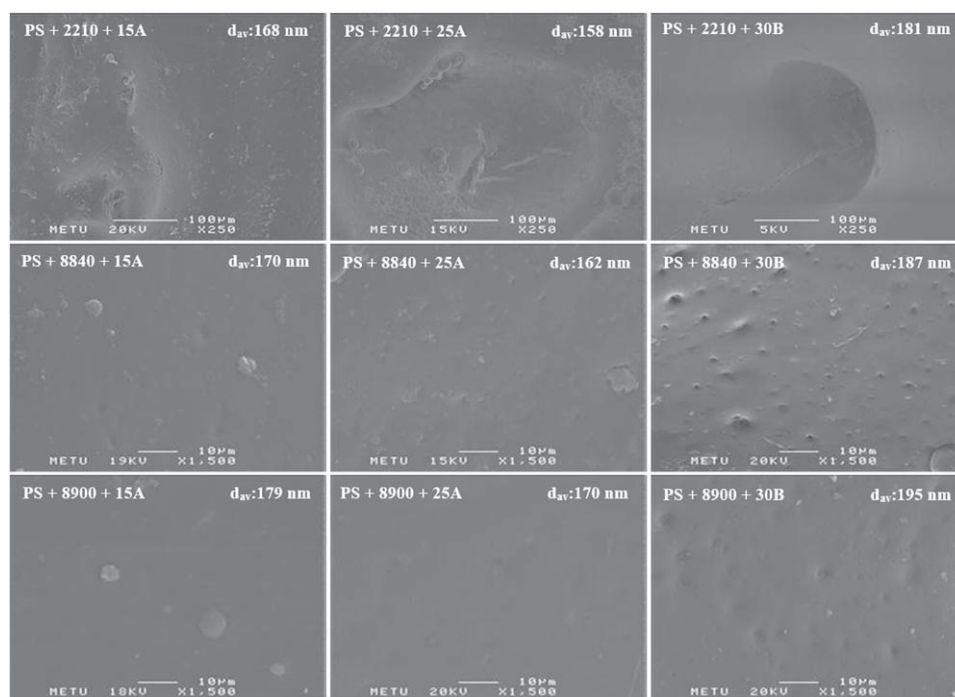


Figure 3. SEM images of the nanocomposites.

elastomeric phase in the PS matrix. In order to obtain accurate results, about 50–100 domains of the elastomeric phase were analyzed and the average domain sizes ( $d_{av}$ ) of each sample were calculated. The calculated  $d_{av}$  values are indicated on the SEM photographs for each sample as displayed in figure 3. The spherical domains in the PS matrix are formed from the dispersed droplets of the elastomers. The domain sizes range between 150–195 nm. According to SEM images, clay particles mostly reside at the interphase between PS and elastomeric domains. Since the elastomeric phase has higher viscosity than the PS matrix, its presence increases the viscosity of the blend and the shear stress applied on the clay platelets during extrusion [28]. However, increasing viscosity also prevents the dispersion of elastomeric phase into small droplets, because the shear stress that is applied on to the material becomes insufficient.

TEM images of the ternary nanocomposites containing organoclay are shown in figure 4. According to the TEM images, dispersion of the clay layers is improved in the presence of the elastomeric compatibilizers. Intercalated structure of the clay platelets is obtained in the nanocomposites containing elastomers.

### 3.3. Melt flow index measurements

MFI test was performed to investigate the flow behavior of the materials. MFI value depends on many parameters such as viscosity of the material, molecular weight of the material, degree of chain branching, the presence of co-monomers and heat transfer. MFI values of the samples are shown in table 2. All of the elastomeric materials have lower MFI values than PS. Addition of elastomer and organoclay caused reduction in MFI values. The binary nanocomposites have lower MFI (higher viscosity) than the neat PS, owing to the filler effect of the organoclays. Rigid fillers are known to increase the viscosity of polymer melts according to the literature [29–32].

### 3.4. Tensile tests

Effects of montmorillonite type on the tensile properties of PS are shown in figure 5. There is no significant improvement in the tensile strength and elongation at break values of the neat polymer by producing binary nanocomposites. Young's modulus of unfilled PS increases with the addition of organoclays. The highest tensile strength and modulus values were observed for Cloisite® 30B containing sample among the binary composites. Figure 6 shows the tensile properties of the ternary nanocomposites prepared with the elastomers and organoclays. The sample PS + 8900 + 30B yields significant improvement for the tensile strength of unfilled PS, whereas no obvious changes for other compositions were observed in the case of tensile strength. It should be noted that this ternary nanocomposite exhibited the highest intercalation as observed by XRD analysis. Addition of organoclay+elastomer increases the elongation at break of the ternary composites according to figure 6. Young's modulus of PS exhibits reduction with the additions of elastomers and organoclays with the exception

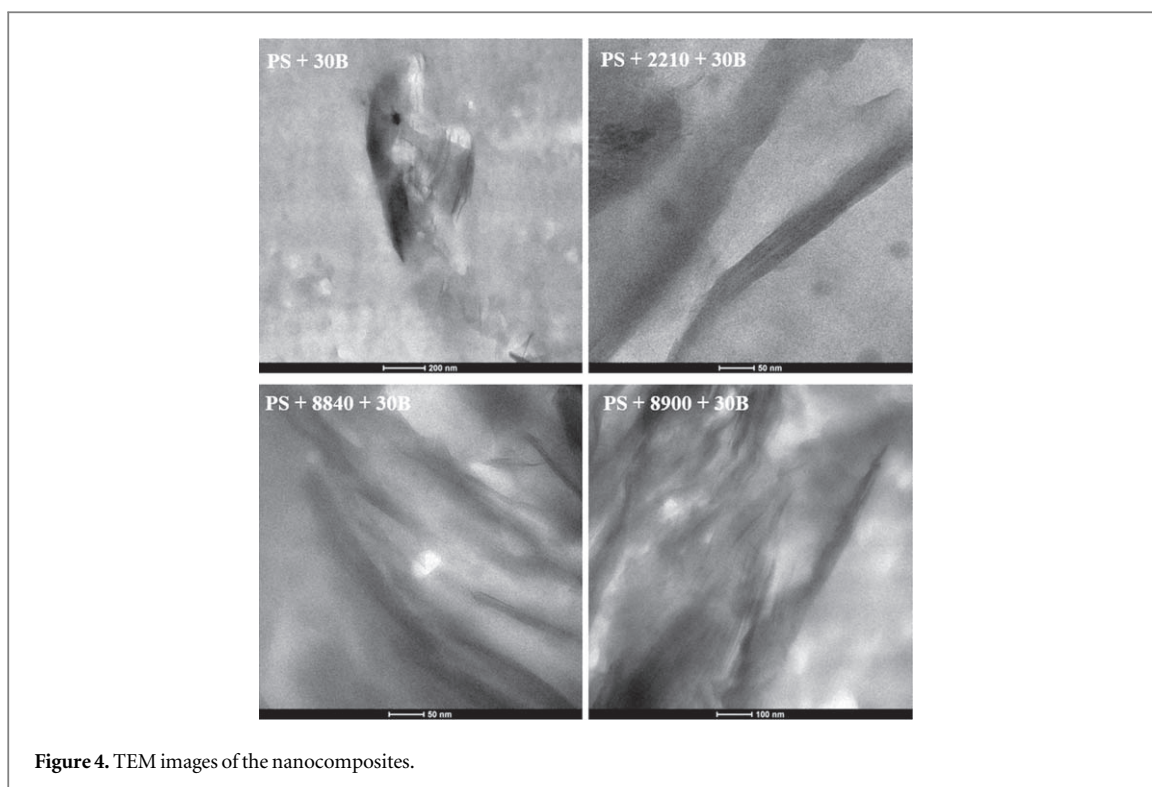


Figure 4. TEM images of the nanocomposites.

Table 2. MFI test results.

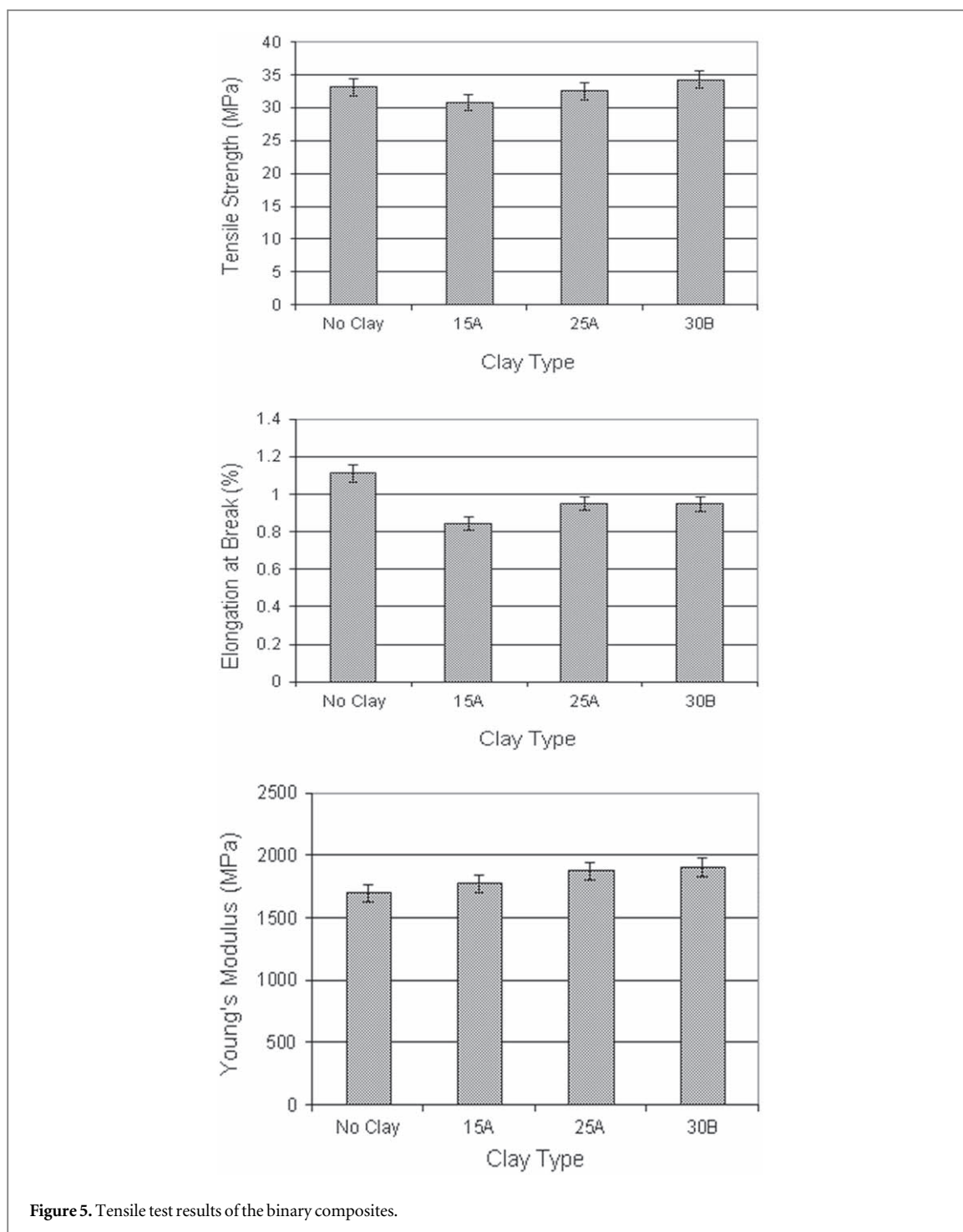
Composition	MFI (g/10 min)
PS	20.4 ± 0.1
2210	3.6 ± 0.1
8840	6.1 ± 0.2
8900	7.6 ± 0.1
PS + 15 A	16.6 ± 0.2
PS + 25 A	15.0 ± 0.1
PS + 30B	16.9 ± 0.1
PS + 2210 + 15 A	15.4 ± 0.1
PS + 2210 + 25 A	14.8 ± 0.2
PS + 2210 + 30B	15.9 ± 0.1
PS + 8840 + 15 A	17.1 ± 0.2
PS + 8840 + 25 A	17.4 ± 0.2
PS + 8840 + 30B	16.8 ± 0.1
PS + 8900 + 15 A	18.1 ± 0.2
PS + 8900 + 25 A	17.7 ± 0.1
PS + 8900 + 30B	17.3 ± 0.2

of the sample PS + 8840 + 25 A which gives the highest modulus value as compared to PS and other composites.

### 3.5. Impact test

Effect of elastomer type on the impact strength of PS is shown in figure 7. Clay addition makes the polymer stiffer and may reduce the impact strength. However, addition of clay and elastomer together makes the polymer tougher and increases the impact strength. This situation can be explained by the effect of clay particles on the elastomeric domain sizes [33–35]. Elastomeric domains absorb the impact energy and restrict the propagation of the cracks. The highest improvement on impact strength is observed for compositions with Lotader® AX8900. The sample PS + 8900 + 30B exhibits the highest impact strength. Lotader® AX8900 contains the reactive group of glycidyl methacrylate which promotes the elastomer to interact with hydroxyl group of Cloisite 30B.





### 3.6. DSC analysis

In order to observe the effects of organoclay and elastomer additions on the thermal properties of blends and nanocomposites prepared in this study, DSC tests were performed. By this analysis, glass transition temperature ( $T_g$ ) was measured and the data obtained are shown in table 3. According to these data, organoclay additions shift  $T_g$  of unfilled PS to higher temperatures. Segmental motion of the PS chains may be prevented by the intercalated or exfoliated clay layers and this may lead to increase in  $T_g$  values [36–40]. On the other hand, addition of elastomers yields slightly lower  $T_g$  values with respect to the  $T_g$  of PS. These reductions may stem from the high molecular mobility of the elastomeric chains.

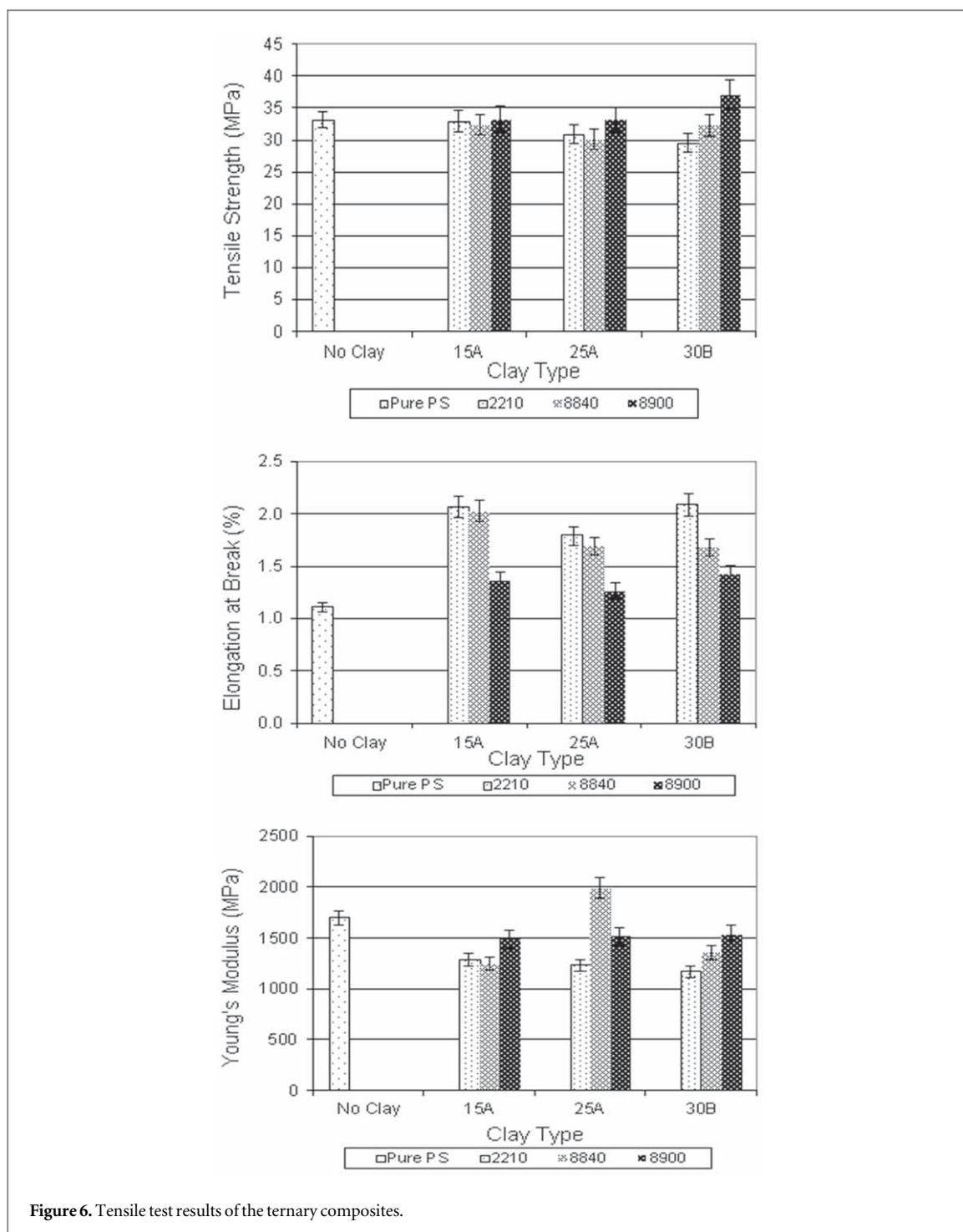


Figure 6. Tensile test results of the ternary composites.

#### 4. Conclusions

In this study, aliphatic elastomers, Lotader AX8900, AX8840 and 2210 were used as the compatibilizer phase. Blending of the elastomer and PS was done by a co-rotating twin screw extruder. As observed from SEM analysis, clay particles mostly reside at the interphase between PS and the elastomeric domains. The composites exhibit lower MFI values as compared to the unfilled PS. Tensile test results show that, combination of 30B and AX8900 gives the highest tensile strength and modulus values among the compositions investigated. Elastomer addition leads to significant increase in elongation of PS. Organoclay + elastomer additions mostly cause improvement for the impact strength of PS. AX8900 containing sample gives the highest impact strength value among all the composites. When the results of DSC analysis are investigated, increase in the  $T_g$  of PS is observed with the addition of organoclays. Elastomer containing samples display relatively lower  $T_g$  values.

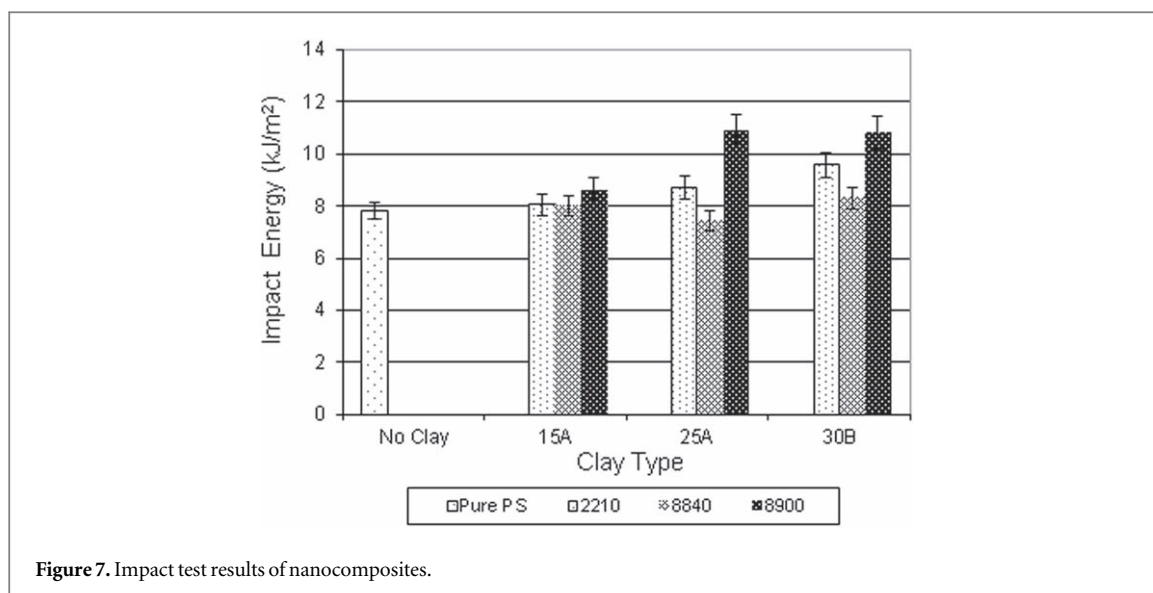


Figure 7. Impact test results of nanocomposites.

Table 3. DSC test results.

Composition	$T_g$ (°C)
PS	107.8
PS + 15 A	108.7
PS + 25 A	108.9
PS + 30B	108.8
PS + 2210 + 30B	107.4
PS + 8840 + 30B	107.6
PS + 8900 + 30B	107.3

## Acknowledgments

This study was supported by The Scientific and Technological Research Council of Turkey under grant no. TUBITAK 106T425.

## ORCID iDs

Ali Sinan Dike  <https://orcid.org/0000-0001-6214-6070>

## References

- [1] Callister W D 1997 *Material Science and Engineering: An Introduction* 6th Ed (New York: Wiley)
- [2] Kroschwitz J I and Mark H F 2003 *Encyclopedia of Polymer Science and Technology* 3rd Ed (New York: Wiley Interscience)
- [3] Zanetti M, Lomakin S and Camino G 2000 Polymer layered silicate nanocomposites *Macromol. Mater. Eng.* **279** 1
- [4] Giannelis E P 1996 Polymer layered silicate nanocomposites *Adv Mater* **8** 29
- [5] Vaia R A, Ishii H and Giannelis E P 1993 Synthesis and properties of two dimensional nanostructures by direct intercalation of polymer melts in layered silicates *Chem. Mater.* **5** 1694
- [6] Ray S S and Okamoto M 2003 Polymer/layered silicate nanocomposites: A review from preparation to processing *Prog. Polym. Sci.* **28** 1539
- [7] Wan Y *et al* 2019 A review of recent advances in two-dimensional natural clay vermiculite-based nanomaterials *Mater. Res. Express* **6** 102002
- [8] Pavlidou S and Papaspyrides C D 2008 A review on polymer-layered silicate nanocomposites *Prog. Polym. Sci.* **33** 1119
- [9] Ebewele R O 2000 *Polymer Science and Technology* (USA: CRC Press LLC)
- [10] Scheirs J and Priddy D 2003 *Modern Styrenic Polymers: Polystyrenes and Styrenic Copolymers* (New York: Wiley)
- [11] Rubin I I 1990 *Handbook of Plastic Materials and Technology* (New York: Wiley)
- [12] Park C I *et al* 2004 Thermal and mechanical properties of syndiotactic polystyrene/organoclay nanocomposites with different microstructures *J. Polym. Sci., Part B: Polym. Phys.* **42** 1685
- [13] Zhang W A *et al* 2003 Influence of four different types of organophilic clay on the morphology and thermal properties of polystyrene/clay nanocomposites prepared by the  $\gamma$ -ray radiation technique *Eur. Polym. J.* **39** 2323
- [14] Xie W *et al* 2003 A study of the effect of surfactants on the properties of polystyrene-montmorillonite nanocomposites *Polym. Eng. Sci.* **43** 214

- [15] Tanoue S *et al* 2006 Effect of screw rotation speed on the properties of polystyrene/organoclay nanocomposites prepared by a twin-screw extruder *J. Appl. Polym. Sci.* **101** 1165
- [16] Doh J G and Cho I 1998 Synthesis and properties of polystyrene-organoammonium montmorillonite hybrid *Polym. Bull.* **41** 511
- [17] Gilman J W *et al* 2000 Flammability properties of polymer-layered silicate nanocomposites, polypropylene and polystyrene nanocomposites *Chem. Mater.* **12** 1866
- [18] Fu X and Qutubuddin S 2000 Synthesis of polystyrene-clay nanocomposites *Mater. Lett.* **42** 12
- [19] Zhang J and Wilkie C A 2004 A carbocation substituted clay and its styrene nanocomposite *Polym Degrad Stabil* **83** 301
- [20] Brindley G W and Brown G 1980 *Crystal Structures of Clay Minerals and their x-ray Identification* (London: Mineralogical Society)
- [21] Lee K M and Han C D 2003 Rheology of organoclay nanocomposites: Effects of polymer matrix/organoclay compatibility and the gallery distance of organoclay *Macromolecules* **36** 7165
- [22] Alexandre M and Dubois P 2000 Polymer-layered silicate nanocomposites: Preparation, properties, and uses of a new class of materials *Mater. Sci. Eng.* **28** 1
- [23] Tayfun U and Dogan M 2016 Improvement the dyeability of poly(lactic acid) fiber using organoclay during melt spinning *Polym. Bull.* **73** 1581
- [24] Moore D M and Reynolds R C 1997 *X-ray Diffraction and the Identification and Analysis of Clay Analysis of Clay Minerals* (Oxford: Oxford University Press)
- [25] Dike A S and Yilmazer U 2019 Improvement of organoclay dispersion into polystyrene-based nanocomposites by incorporation of SBS and maleic anhydride-grafted SBS *J. Thermoplast. Compos. Mater.* [Epub Online](#)
- [26] Chiu C W *et al* 2014 Intercalation strategies in clay/polymer hybrids *Prog. Polym. Sci.* **39** 443
- [27] Dike A S 2011 Nanocomposites based on blends of polystyrene *PhD Thesis* Middle East Technical University, Ankara, Turkey
- [28] Yeniova C E and Yilmazer U 2013 Effect of different types of organoclays and compatibilizers on the properties of polystyrene-based nanocomposites *J. Appl. Polym. Sci.* **127** 3673
- [29] Xiao C *et al* 2017 Synergistic effect of selectively distributed AlN/MWCNT hybrid fillers on the morphological, mechanical and thermal properties of polycarbonate/maleated poly[styrene-b-(ethylene-co-butylene)-b-styrene] triblock copolymer (SEBS-g-MA) composites *Mater. Res. Express* **4** 025101
- [30] Kanbur Y and Tayfun U 2019 Development of multifunctional polyurethane elastomer composites containing fullerene: Mechanical, damping, thermal, and flammability behaviors *J Elastom Plast* **51** 262
- [31] Othman M H *et al* 2018 The optimisation of processing condition for injected mould polypropylene-nanoclay-gigantochloa scortechinii based on melt flow index *IOP Conf. Ser.: Mater. Sci. Eng.* **324** 012073
- [32] Alghadi A M, Tirkes S and Tayfun U 2020 Mechanical, thermo-mechanical and morphological characterization of ABS based composites loaded with perlite mineral *Mater. Res. Express* **7** 015301
- [33] Borggreve R J M, Gaymans R J and Schuijjer J 1989 Impact behaviour of nylon-rubber blends: 5. Influence of the mechanical properties of the elastomer *Polymer* **30** 71
- [34] Ozkoc G, Bayram G and Bayramli E 2004 Effects of polyamide 6 incorporation to the short glass fiber reinforced ABS composites: An interfacial approach *Polymer* **45** 8957
- [35] Savas L A, Tayfun U and Dogan M 2016 The use of polyethylene copolymers as compatibilizers in carbon fiber reinforced high density polyethylene composites *Compos Part B Eng* **99** 188
- [36] Gilissen K *et al* 2014 Influence of the epoxidation degree of a polystyrene-polybutadiene-polystyrene (SBS) triblock copolymer on the compatibilization with an organomodified nanoclay *J. Mater. Sci.* **49** 3622
- [37] Eselini N *et al* 2019 Production and characterization of poly(lactic acid)-based biocomposites filled with basalt fiber and flax fiber hybrid *J. Elastom Plast* [Epub Online](#)
- [38] Seyidoglu T and Yilmazer U 2015 Modification and characterization of bentonite with quaternary ammonium and phosphonium salts and its use in polypropylene nanocomposites *J. Thermoplast. Compos. Mater.* **28** 86
- [39] Savas L A *et al* 2017 Effect of carbon fiber amount and length on flame retardant and mechanical properties of intumescent polypropylene composites *J. Compos. Mater.* **52** 519
- [40] Donnet J B 2013 Nano and microcomposites of polymers elastomers and their reinforcement *Compos. Sci. Technol.* **63** 1085